Journal of Physics: Conference Series **500** (2014) 162005 doi:10.1088/1742-6596/500/16/162005

Density functional theory investigation of sodium azide at high pressure

B A Steele, A C Landerville and I I Oleynik

Department of Physics, University of South Florida, 4202 East Fowler Ave., Tampa, FL 33620

E-mail: brad4@mail.usf.edu

Abstract. High pressure experiments utilizing Raman spectroscopy indicate that the α phase of sodium azide undergoes a polymeric phase transition at high pressure. In this work, the structural and vibrational properties, including the first order Raman and infrared spectra, of the α phase of sodium azide are calculated using first-principles density functional theory up to 92 GPa. The equation of state of $\alpha-NaN_3$ is obtained within the quasi-harmonic approximation at various temperatures. Each Raman-active mode blue shifts under compression whereas the doubly degenerate IR-active azide bending mode red-shifts under compression. However, at 70 GPa, the intensity of the B_u IR-active bending mode decreases substantially, and a new distorted azide bending lattice mode appears in the IR spectrum. In contrast to the bending mode, this new mode blue-shifts under compression. No new modes appear in the Raman spectra at high pressure, indicating that the changes in the Raman spectrum seen in experiment at high pressure are signs of new high nitrogen content structures, but not due to sodium azide.

1. Introduction

All-nitrogen non-molecular solids attracted substantial interest during the last several decades [1, 2, 3, 4, 5, 6] due to their potential use as a powerful energetic material (EM). Measurements of the Raman spectrum at high pressures and temperatures indicate the possible formation of a non-molecular phase of nitrogen when using sodium azide (NaN_3) as a precursor material [7, 8, 9]. Hexagonal $\beta - NaN_3$ is the ground state crystal structure at room temperature and ambient pressure and is composed of parallel planes of N_3^- ions that are directed perpendicular to planes of sodium ions in the $R\bar{3}m$ space group. $\beta - NaN_3$ undergoes a polymorphic phase transition to the $\alpha - NaN_3$ phase at 0.25 GPa [12]. The $\alpha - NaN_3$ structure features parallel planes of N_3^- ions which are rotated to make an angle $\neq 90^\circ$ with the planes of sodium ions, resulting in a crystal structure with the C2/m space group symmetry [10]. When hydrostatically compressed to pressures greater than 15 GPa, several new peaks appear in the experimental Raman spectrum [7], in addition to those observed at low pressure [11, 13]. At pressures exceeding 50 GPa, even more modes appear in the Raman spectra that are believed to be the result of a polymeric form of nitrogen [7]. Therefore the important question arises whether these new peaks are indeed due to the appearance of a new polymeric species of pure nitrogen or due to new phases of NaN_3.

In this work, the structural and vibrational properties of the α-phase of sodium azide are examined up to 92 GPa using first principles density functional theory calculations. A focus is made on the α-phase, and not the β-phase, because the $\beta - \alpha$ phase transition occurs at just 0.25 GPa at room temperature and persists up to at least 15 GPa [12]. The equilibrium volume


Content from this work may be used under the terms of the Creative Commons Attribution 3.0 licence. Any further distribution of this work must maintain attribution to the author(s) and the title of the work, journal citation and DOI.
Published under licence by IOP Publishing Ltd

and Raman spectrum at ambient conditions are compared to experimental data to verify the accuracy of the calculations before Raman spectrum predictions are made at high pressures.

2. Computational Details

First-principles density functional theory (DFT) calculations are performed using the Perdew-Burke Ernzerhof (PBE) generalized gradient approximation (GGA) to DFT [14] as implemented in the plane-wave Quantum Espresso package. Norm-conserving pseudopotentials are used. Since currently available DFT functionals poorly represent long range van der Waals (vdW) interactions, the empirical dispersive correction by Grimme [15] is added on. A comparison between pure PBE and PBE with vdW is provided to demonstrate that the vdW corrections are necessary to achieve a better agreement with experiment. To avoid any artificial forces caused by the switching function employed in the empirical Grimme scheme, DFT without vdW correction is employed to obtain vibrational properties. The Raman spectrum depends on second derivatives of the electronic density [16], therefore, it must be calculated accurately, which requires a large energy cutoff and dense k-point sampling. Specifically, 140 Ry energy cutoff and 0.05 Å^{-1} k-point sampling are used to achieve good accuracy of calculated Raman spectra. The equilibrium volume is obtained by optimization of atomic coordinates and cell parameters to achieve zero force on each atom and the zero components of the stress tensor.Thermodynamic properties are calculated within the Quasi Harmonic Approximation (QHA) by including the contribution to the free energy from the normal mode vibrations. Within the QHA, the pressure is a sum of three terms: the cold pressure due to compression of the crystal lattice, the zero point energy and the thermal contributions to the pressure. The vibrational spectrum is computed using density functional perturbation theory (DFPT) [17], which allows for analytic calculation of the second derivatives of the total energy with respect to atomic displacements within the linear response framework to obtain the dynamical matrix. Similarly, derivatives with respect to applied electric fields are computed using linear response theory to determine the Raman intensities [16, 18]. Note that such calculations of spectra do not take into account anharmonic effects such as overtones and mode coupling.

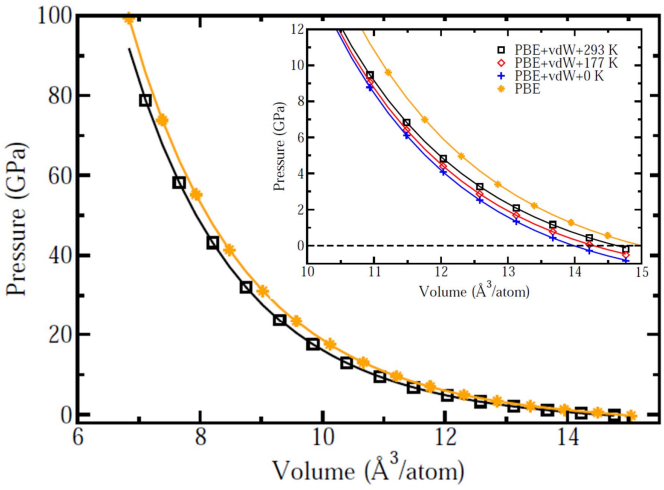

Figure 1. Equation of state of $\alpha - NaN_3$ calculated at various temperatures with and without the the van der Waals correction.

Table 1. A comparison between the calculated and experimental equilibrium volume, bulk modulus, and it's pressure derivative of $\alpha - NaN_3$.

Method	V_0(Å^3/atom)	B_0(GPa)	B_0'
PBE+vdW+0 K	13.98	17.53	5.84
PBE+vdW+293 K	14.64	13.78	5.93
PBE	14.99	14.06	5.94
Exp. at 293 K [12]	14.59	17.10	5.70

3. Results and Discussion

3.1. Structural properties of α-NaN_3 under compression

The structural properties of $\alpha - NaN_3$ are calculated as a function of pressure. The isothermal equation of state (EOS) is shown in figure 1 which compares the pressure versus volume dependence calculated with the pure PBE functional at 0 K and that calculated using the PBE functional with Grimme's vdW correction at 293 K.

The insert shows PBE+vdW $P(V)$ calculated at 0 K, 177 K and 293 K. The pressure vs volume dependence is fitted in the pressure range 0-11 GPa using a third order Birch-Munaghan (BM) EOS to determine the bulk modulus B_0 and its pressure derivative $B_0^{'}$. The results of the fit are shown in table 1, which compares the calculated V_0, B_0 and $B_0^{'}$, with those from experiment [12]. The equilibrium volume V_0 obtained from the BM fit is in very good agreement with V_0 obtained independently during structure optimization at $P = 0$ GPa.

The equilibrium volume V_0 of the α-phase calculated at zero temperature is 4.2% less than the experimental volume measured at room temperature [12]. This error is expected to be due to thermal expansion, which is not taken into account in "cold" DFT calculations. Therefore, once the effect of finite temperature calculated within QHA is taken into account, the theoretical equilibrium volume is just 0.3 % more than the experimental value for α-NaN_3; see table 1. On the other hand the equilibrium volume calculated without vdW and the QHA is 2.7 % greater than in experiment, which demonstrates the importance of proper accounting for finite temperature and vdW interactions in DFT calculations.

Because of their linear geometry, the orientation of the azides plays an important role in response of NaN_3 to hydrostatic compression. Figure 2(a) displays the behavior of lattice constants upon compression. The a and b lattice constants lie in the sodium ion plane, whereas the azides are directed perpendicular to the b axis and at a (small) angle to the c axis. The angle the azides make with the c axis behaves similar to how the monoclinic angle β changes under compression (figure 2(b)). It reduces significantly up to 15 GPa, then doesn't change much upon further compression. As this angle increases, the azides are directed more towards the a axis at higher pressures. This causes the a lattice constant to decrease less than b at higher pressures. In addition, since the azides lie mostly along the c axis, the c lattice constant does not change much with compression.

3.2. Raman and IR spectra of α-NaN_3 as a function of pressure

The evolution of the Raman spectrum as a function of pressure is shown in figure 3. Assuming that the vibrational frequencies are dependent on volume only, the pressure dependent Raman and IR spectra are calculated using the PBE GGA functional without vdW contributions and 0 K at volumes matching those calculated with vdW and specific temperature and pressure. Excellent agreement with experiment performed at zero pressure and 100 K [13] is achieved for the frequency of the intra-molecular azide symmetric stretch (A_g) Raman active mode, which is predicted to be 1,363 cm^{-1}, see figure 3. This means the predicted frequency is within 0.1%

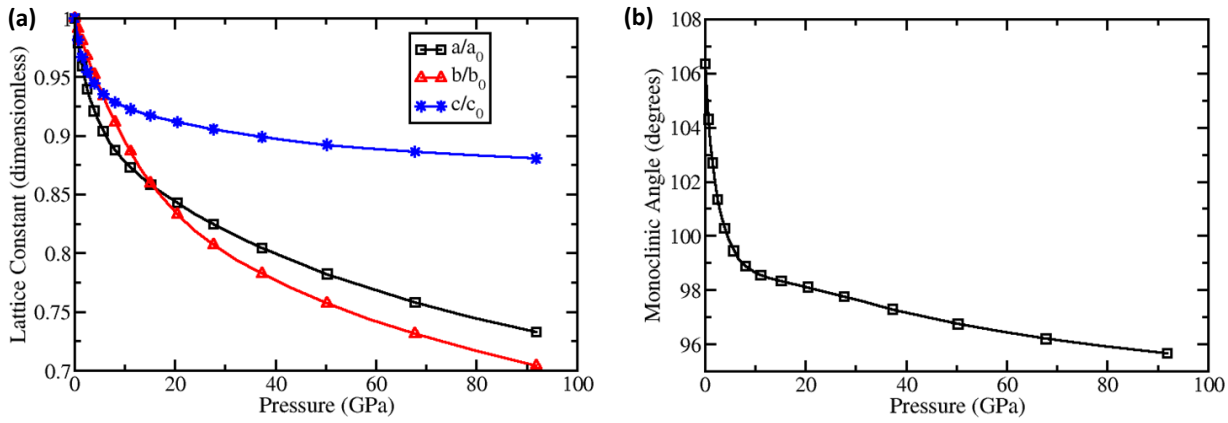

Figure 2. (a) Pressure dependence of the normalized lattice parameters $a_0 = 6.16$ Å, $b_0 = 3.67$ Å, and $c_0 = 5.22$ Å(b) and the monoclinic angle, β of $\alpha - NaN_3$.

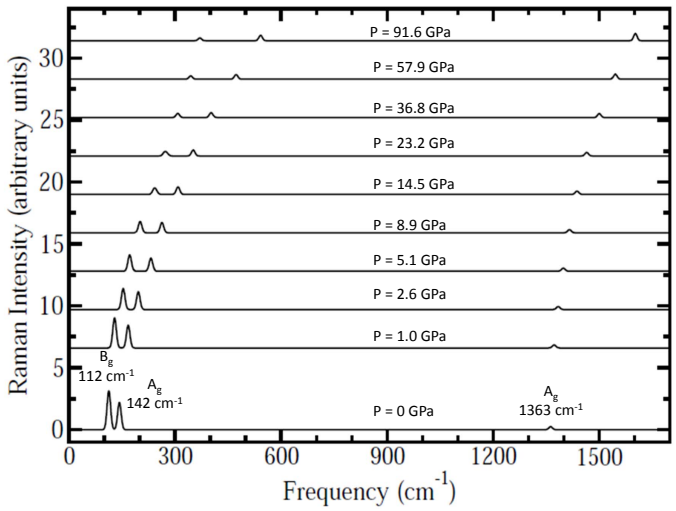

Figure 3. The evolution of the calculated Raman spectra of the α-phase of sodium azide under compression at 100 K. Experimental frequencies at zero pressure are 127 cm^{-1}, 146 cm^{-1}, and 1,363 cm^{-1} [13].

of the experimental value. The low frequency modes reflect the weak intra-molecular vdW interactions that currently avaiable functionals poorly represent in DFT; hence, the computed low frequency inter-molecular modes are less accurate than the intra-molecular modes. The N_3^- librational modes are predicted to have frequencies of 112 cm^{-1} and 142 cm^{-1} for the B_g and A_g librons respectively, see figure 3. These modes have been experimentally measured by Iqbal [13] to have frequencies of 127 cm^{-1} and 146 cm^{-1} respectively at 100 K and $P = 0$ GPa, which differ by -11.8% and -2.7% from the calculated frequencies respectively. The difference may be an effect of anharmonicity in the modes, as well as vdW interactions which are not included in the phonon calculation. The relative intensities of the modes are in agreement with experiment, with the B_g mode being the most intense peak in the spectrum at low pressure (figure 3). Each Raman-active mode blue shifts to higher frequencies under compression, see figure 3.

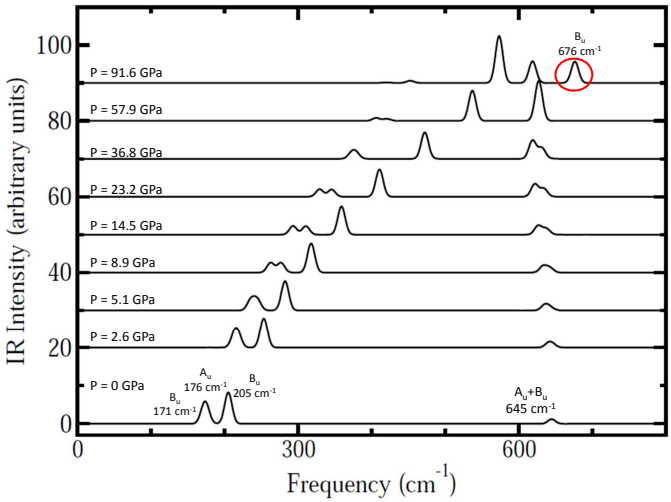

Figure 4. Evolution of the low-frequency IR-active modes of the α-phase of sodium azide under compression at 100 K.

The evolution of the low frequency IR-active modes under compression is shown in figure 4. At a pressure of 0 GPa, the lattice IR modes have frequencies of 171 cm^{-1}, 176 cm^{-1}, and 205 cm^{-1}; the doubly degenerate azide bending mode has a frequency of 645 cm^{-1}; and the asymmetrical azide stretch has a frequency of 2,168 cm^{-1}. To the author's knowledge, experimental measurements on the IR-modes have only been performed on β-NaN_3 and not α-NaN_3. Only two lattice modes are visible in the IR-spectrum because the B_u (171 cm^{-1}) and A_u (176 cm^{-1}) lattice modes overlap. These two modes involve displacements in the x and y directions respectively. The doubly degenerate bending mode, labeled as A_u+B_u in figure 4, red-shifts under compression, then splits at about 70 GPa into a new lattice mode and the A_u bending mode. The splitting is visible in the panel of figure 4 corresponding to pressure 91.8 GPa. At this pressure, the B_u (xz) bending mode, shown in figure 5(a), becomes much less intense and disappears entirely from the spectrum. A new lattice mode, depicted in figure 5(b), appears. It has the same B_u symmetry as the bending mode and involves a distorted azide bending. Contrary to the bending mode, this new mode blue shifts under compression. It is a lattice mode as it involves a concerted translation of the sodium ion sublattice and the two end nitrogen atoms of azide N_3^- along the crystallographic c-axis. This is most likely due to the electrostatic attraction between the negatively charged end-nitrogen atoms and the positively charged sodium atoms, which is enhanced at higher pressures.

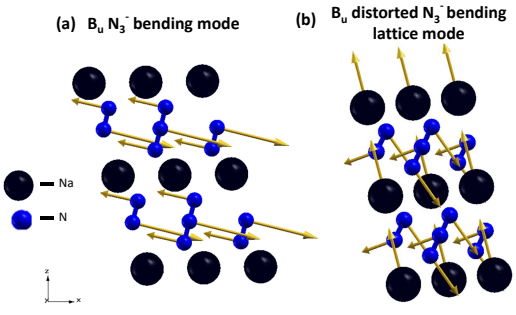

Figure 5. (a) The bending mode (B_u) in the xz-plane at equilibrium conditions and (b) a lattice mode that becomes IR-active at at 91.6 GPa.

4. Conclusions

The equation of state and the Raman and IR spectrum have been calculated for $\alpha - NaN_3$ under hydrostatic compression up to 92 GPa. The calculated equilibrium volume is less than 1% of experimental values if the thermal expansion of the crystal is taken into account using the QHA. The calculated frequencies of the internal modes are in excellent agreement with experiment, while the lower frequency librational modes differ from experiment by about 10 %. It is found that for $\alpha - NaN_3$ at about 70 GPa, the IR-active bending mode disappears and a new lattice mode appears in the spectrum that blue-shifts under compression. The new lattice mode involves displacements along the c-axis as well as a distorted azide bending. No new modes appear in the Raman spectra at high pressure, indicating that the changes in the Raman spectrum seen in experiment at high pressure are signs of new high nitrogen content structures, but not due to sodium azide.

Acknowledgements

The authors thanks Jonathan Crowhurst at LLNL and Su Peiris at DTRA for enlightening discussions. This research is supported by Defense Threat Reduction Agency, grant # HDTRA1-12-1-0023.

References

[1] Martin R M and Needs R J 1986 *Phys. Rev.* B **34** 5082–5092
[2] Mailhiot C, Yang L and McMahan A 1992 *Phys. Rev.* B **46** 14419–14435
[3] Eremets M I, Gavriliuk A G, Trojan I A, Dzivenko D A and Boehler R 2004 *Nature Mater.* **3** 558–63
[4] Eremets M I, Gavriliuk A G and Trojan I A 2007 *Appl. Phys. Lett.* **90** 171904
[5] Pickard C and Needs R 2009 *Phys. Rev. Lett.* **102** 125702
[6] Wang X, Tian F, Wang L, Cui T, Liu B and Zou G 2010 *J. Chem. Phys.* **132** 024502
[7] Eremets M I, Popov M Y, Trojan I A, Denisov V N, Boehler R and Hemley R J 2004 *J. Chem. Phys.* **120** 10618–23
[8] Crowhurst J C, Manaa M R, Zaug J M and Goncharov A F 2010 *Towards new energy-rich molecular systems: Polynitrogen, Proc. of the 14^{th} Int. Det. Symp.* (Coeur d'Alane) p 829
[9] Peiris S M and Russell T P 2003 *J. Phys. Chem.* A **107** 944–947
[10] Pringle G E and Noakes D E 1968 *Acta Crystallogr. Sect.* B **24** 262–269
[11] Simonis G J and Hathaway C E 1974 *Phys. Rev.* B **10** 4419–4433
[12] Zhu H, Zhang F, Ji C, Hou D, Wu J, Hannon T and Ma Y 2013 *J. Appl. Phys.* **113** 033511
[13] Iqbal Z 1973 *J. Chem. Phys.* **59** 1769
[14] Perdew J, Burke K and Ernzerhof M 1996 *Phys. Rev. Lett.* **77** 3865–3868
[15] Grimme S 2006 *J. Comp. Chem.* **27** 1787–1799
[16] Lazzeri M and Mauri F 2003 *Phys. Rev. Lett.* **90** 036401
[17] Baroni S, Gironcoli S D, Corso A D, Scuola S, Superiore I, Istituto I, Materia F, Trieste I and Giannozzi P 2001 *Rev. Mod. Phys.* **73** 515
[18] Porezag D and Pederson M R 1996 *Phys. Rev.* B **54** 7830–7836
[19] Zhu W, Xiao J and Xiao H 2006 *J. Phys. Chem.* B **110** 9856–62